Annals of Glaciology 31 2000

Tidewater glaciers: frontal flow acceleration and basal sliding

Andreas Vieli,[1,2] Martin Funk,[2] Heinz Blatter[1]
[1]*Geographisches Institut,* Eidgenössische Technische Hochschule, Winterthurerstrasse 190, CH-8057 Zürich, Switzerland*
[2]*Versuchsanstalt für Wasserbau, Hydrologie und Glaziologie, ETH Zentrum, Gloriastrasse 37/39, CH-8092 Zürich, Switzerland*

ABSTRACT. A numerical glacier-flow model (finite-element method) is used to suggest the processes that control the flow behind the calving front of a tidewater glacier. The model is developed for grounded calving glaciers and includes an effective-pressure-dependent sliding law. The sliding law is implemented by adding a soft basal layer with a variable viscosity. The model is applied on Hansbreen, a tidewater calving glacier in Svalbard. Comparison between modeled surface velocities and observed velocity data shows good agreement. We conclude that the flow of a grounded calving glacier can be modeled with an effective-pressure-dependent sliding law.

INTRODUCTION

The flow dynamics of tidewater calving glaciers is of great interest but poorly understood (Meier, 1994; Van der Veen, 1996). Increasing surface flow velocities towards the calving front have been observed on several grounded calving glaciers, including Hansbreen, Spitsbergen; Columbia Glacier, Alaska (Krimmel and Vaughn, 1987); Glaciar Moreno, Patagonia (Rott and others, 1998); and Nordbogletscher, Greenland (Funk and Bösch, 1990). Understanding the processes controlling the flow field behind a calving front is essential for developing a physically based model for calving. It is known that basal sliding strongly affects the flow of grounded calving glaciers (Kamb and others, 1994; Meier and others, 1994; Van der Veen, 1996). Effective pressure (ice-overburden minus water pressure) is suggested as one important controlling factor for basal sliding (Iken, 1978; Budd and others, 1979; Bindschadler, 1983).

This study concentrates on Hansbreen, a grounded calving glacier in Svalbard, for which an extensive dataset exists. A numerical glacier-flow model, including basal sliding, is used to suggest the important processes that control the flow behind the calving front.

DATABASE AND FIELD OBSERVATIONS

Hansbreen is a tidewater calving glacier situated at Hornsund, southern Spitsbergen. The glacier covers an area of 57 km^2 and is about 16 km long (Fig. 1). It ends in the sea with a 1.3 km wide calving front. The front height above water level is 30–40 m. The glacier bed along the frontal 10 km is below sea level. Since the establishment of the Polish polar station in the vicinity of Hansbreen in 1957, several glaciological investigations have been carried out, and an extensive dataset of Hansbreen is available (Jania and Kaczmarska, 1997). It includes glacier surface topography from photogrammetry, bed topography from radio-echo soundings (Glazovskiy and others, 1991) and depth soundings of the fjord in front of the glacier (Giżejewski, 1997). Furthermore, annually measured frontal positions and sur-

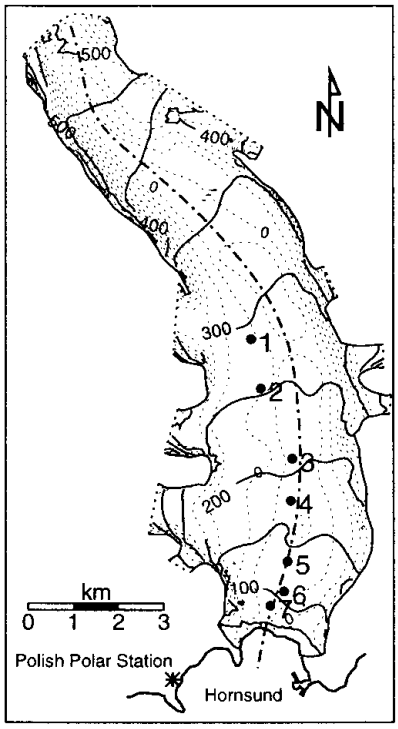

Fig. 1. Map of Hansbreen showing surface (solid contour lines) and bed (dashed contour lines) topography. The contour intervals are 50 m. The location of the stakes, used for velocity measurements by terrestrial survey, are shown with the corresponding stake numbers (1–7) used in the text. The dashed-dotted line indicates the flowline used for the model calculations.

* Now Institute for Climate Research.

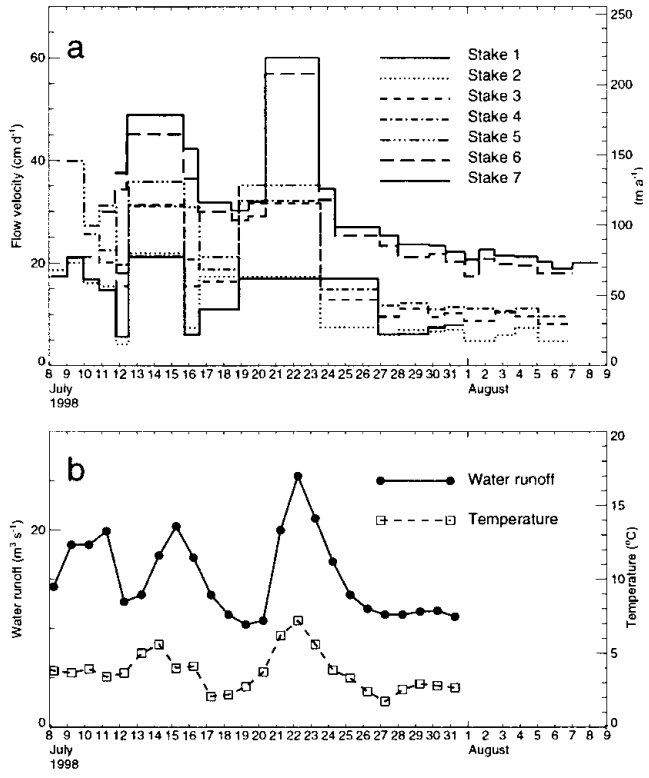

Fig. 2. (a) Variation of flow velocities with time at stakes 1–7 measured by terrestrial survey. (b) Variation with time of mean daily temperature at Hornsund meteorological station, and daily water runoff at neighbouring Werenskjøldbreen.

face velocity data determined by terrestrial photogrammetry are available from 1982 onwards (Jania and Kolondra, 1982; Jania, 1988).

In summer 1998, additional surface velocity measurements were made on Hansbreen by terrestrial survey of seven stakes along a flowline with a temporal resolution of 1–2 days (unpublished information from J. Jania). The velocity data show a high variability in time and space (Fig. 2). Spatially, surface velocity increases significantly towards the calving front, starting 4 km behind the ice cliff (Fig. 5 shown later). Temporally, periods of substantially higher surface velocity were observed to last for 2–3 days (Fig. 2). These "fast-flow" events occurred during periods with significantly higher surface-melt rates. Daily mean temperature recorded at the Hornsund meteorological station of the Institute of Geophysics of the Polish Academy of Science, and water runoff data from the neighboring land-based Werenskjøldbreen (personal communication from M. Pulina, 1998) correlate well with the observed velocity variations (Fig. 2). At the lateral part of the frontal ice cliff, an outflow channel at sea level was observed. During periods with high surface-melt rates, the outflowing water was under high pressure (fountains of water were observed, accompanied by loud noise). The measured fast-flow velocities are mean values taken over a 3 day period. True maximum values are probably higher. The last 10 days of the observation period show relatively constant low velocities. This "slow-flow" period may correspond to a winter flow regime.

Based on extensive studies on valley glaciers, several authors have pointed out that short-term velocity variations are related to changes of basal water pressure (Iken, 1978; Meier and others, 1994; Iken and Truffer, 1997). The observations on Hansbreen suggest that basal sliding predominantly determines the flow field and is affected by variations of surface meltwater production.

MODEL DESCRIPTION

A flow model based on the finite-element method (MARC Analysis Research Corp., 1997) is used. The code solves the full equations for the stress and velocity fields. A two-dimensional version of the model is used to calculate stress and velocity fields along the flowline shown in Figure 1.

Glen's flow law,

$$\dot{\varepsilon}_{ij} = A\tau^{n-1}\tau_{ij}^{n}, \qquad (1)$$

with common values for the flow-law exponent $n = 3$ and the rate factor $A = 0.1\,\mathrm{bar}^{-3}\,\mathrm{a}^{-1}$, has been used in the model (Paterson, 1994). $\dot{\varepsilon}_{ij}$ are the components of the strain-rate tensor, τ_{ij} are the components of the deviatoric stress tensor and τ is the effective stress (second invariant of deviatoric stress tensor).

Basal sliding

The glacier-flow model requires an appropriate boundary condition at the glacier bed to account for basal sliding. We assume a relation between sliding velocity v_b and basal shear traction τ_b of the form:

$$v_\mathrm{b} = c(x)\,\tau_\mathrm{b}^{n'}, \qquad (2)$$

where $c(x)$ is the sliding coefficient and n' is a parameter to be specified (Lliboutry, 1968, 1979).

This relation for basal sliding is implemented in the model by adding a thin soft layer at the glacier base (Leysinger, 1998; personal communication from H. Gudmundsson, 1998) with a flow law corresponding to Equation (1) and with flow parameters n' and A' (Fig. 3). The approach of a different rheology for a subglacial layer has been used before by Alley and others (1987) and MacAyeal (1989) to model ice streams in Antarctica. In both cases the subglacial layer was assumed to be a till layer, and a linear viscous rheology was used. Here the soft layer with a variable viscosity is used as a method to implement the suggested sliding law (Equation (2)) for a given sliding coefficient $c(x)$. The glacier bed corresponds to the interface between glacier ice and the introduced soft layer (Fig. 3). Although the

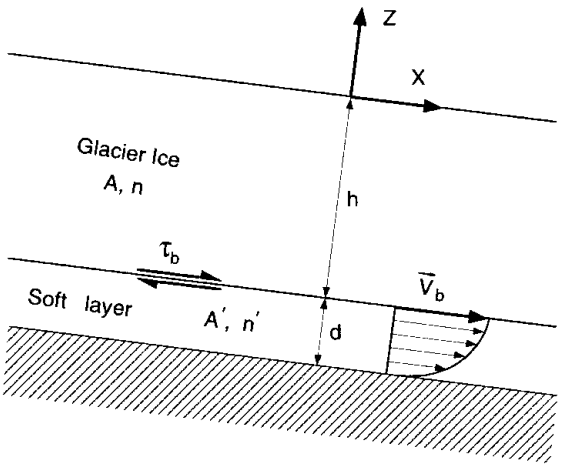

Fig. 3. Schematic view of the glacier, with a soft basal layer for implementing a sliding law that relates the basal velocity $\vec{v}_\mathrm{b}$ to basal shear traction τ_b.

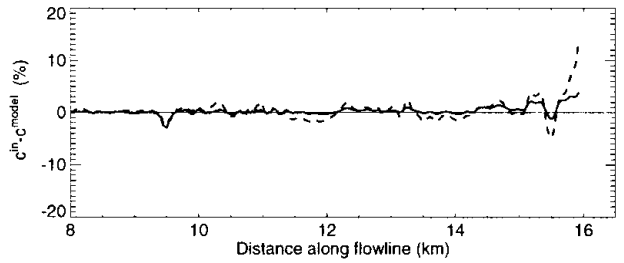

Fig. 4. Difference between input sliding coefficient $c(x)^{\mathrm{in}}$ and calculated sliding coefficient from model results $c(x)^{\mathrm{model}}$ expressed as a percentage of $c(x)^{\mathrm{in}}$ for slow-flow (solid line) and fast-flow (dashed line) scenarios.

physics of the sliding under consideration may not coincide with the soft-slab approach, the described method is mathematically correct. For a prescribed basal boundary condition such as the given sliding law (Equation (2)), the solution for the stress and velocity field is unique (Colinge, 1998).

For an ice slab of thickness h, with an underlying thin soft layer of thickness d and slope angle α, the analytical solution of the basal velocity v_{b} (Fig. 3) in the shallow-ice approximation (Hutter, 1983) is:

$$\begin{aligned} v_{\mathrm{b}} &= \int_{-(h+d)}^{-h} 2A'[\rho g \sin(\alpha) z]^{n'} \, \mathrm{d}z \\ &= 2A'[\rho g \sin(\alpha)]^{n'} \left[h^{n'} d + \frac{n'}{2} h^{n'-1} d^2 + O(d^3) \right]. \end{aligned} \tag{3}$$

With $d \ll h$, terms of order $O(d^2)$ can be neglected and we get

$$v_{\mathrm{b}} \approx 2dA'\tau_{\mathrm{b}}^{n'} \equiv c(x)\tau_{\mathrm{b}}^{n'}, \tag{4}$$

which corresponds to the assumed sliding law (Equation (2)). For the flow model we assume a linear sliding law by setting $n' = 1$. Layer thickness d is constant and $A'(x)$ is given with the sliding coefficient $c(x)$ and is a function of the distance x along the flowline.

Equation (4) is correct for the shallow-ice approximation which neglects longitudinal stress gradients and approximates the basal shear traction with the local driving stress. This may be a poor assumption, especially near the calving front of a tidewater glacier. By using Equation (4) in our model we can estimate the errors due to the said simplification. For a given sliding coefficient $c^{\mathrm{in}}(x) = 2dA'(x)$ we obtain from model calculations the basal shear traction $\tau_{\mathrm{b}}^{\mathrm{model}}$ and basal velocity $v_{\mathrm{b}}^{\mathrm{model}}$ at the upper boundary of the basal layer. Introducing these values into Equation (2) we obtain the sliding coefficient $c^{\mathrm{model}}(x) = v_{\mathrm{b}}^{\mathrm{model}}/\tau_{\mathrm{b}}^{\mathrm{model}}$ which should be identical with $c^{\mathrm{in}}(x)$. While for the shallow-ice approximation $c^{\mathrm{in}}(x)$ is equal to $c^{\mathrm{model}}(x)$, for a real glacier situation these coefficients are different. For a model run of Hansbreen a comparison between c^{in} and c^{model} is shown in Figure 4. The differences are very small in the upper part of the glacier ($<2\%$) and exceed 10% only in the frontmost 300 m.

Basal water pressure and sliding

Basal sliding is strongly affected by changes in water pressure p_{w} (Iken, 1981; Kamb and others, 1994; Meier and others, 1994; Jansson, 1995). For experiments concerned with sliding over a hard bed, Budd and others (1979) proposed a sliding law of the form

$$v_{\mathrm{b}} \propto \tau_{\mathrm{b}}^{m} p_{\mathrm{e}}^{-d}, \tag{5}$$

where p_{e} is the effective pressure (ice-overburden minus water pressure). Bindschadler (1983) successfully applied a similar formula to measured data on glaciers, and Fowler (1987) derived a similar relationship on theoretical grounds. The exponent m is often replaced by Glen's flow-law exponent n, and d is an empirical positive number.

For sliding over a soft glacier bed, Boulton and Hindmarsh (1987) proposed a viscous behaviour for sediment deformation of the form

$$\dot{\varepsilon} \propto \tau^{a} p_{\mathrm{e}}^{-b}, \tag{6}$$

where $\dot{\varepsilon}$ is the strain rate. On the basis of observations, they determined that the exponents were $a = 1.33$ and $b = 1.8$. Expression (6) results in a sliding law analogous to Equation (5). Recent studies suggest that subglacial till behaves like a Coulomb-plastic material (Iverson and others, 1998). Deformation takes place in discrete shear zones whose positions fluctuate with changing basal water pressure. The mean deformation over time conforms very closely to Equation (6).

For the present flow model, we assume a simple sliding law taking into account the effective pressure p_{e} and which is based on current sliding theories. For our model, the sliding coefficient $c(x)$ of Equation (2) is assumed to be:

$$c(x) = q \frac{1}{p_{\mathrm{e}}(x)^{m}}, \tag{7}$$

with the effective pressure $p_{\mathrm{e}}(x) = p_{\mathrm{i}}(x) - p_{\mathrm{w}}(x)$, where $p_{\mathrm{i}}(x)$ is the ice-overburden pressure and $p_{\mathrm{w}}(x)$ is the water pressure at the glacier bed. The parameter m is set to unity, and q is tuned to fit modeled to observed velocities.

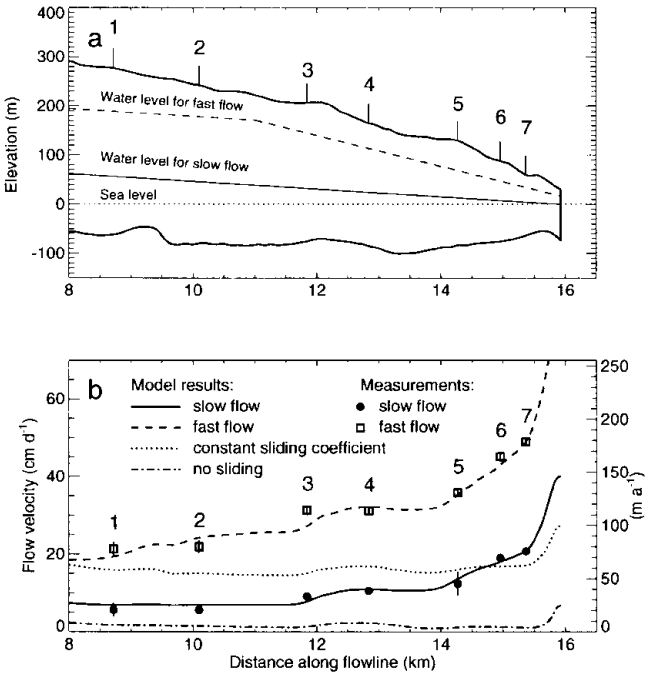

Fig. 5. (a) Profile along the flowline of Hansbreen with glacier bed and surface topography. The lines within the glacier show the assumed water-level scenarios. (b) Measured (symbols) and modeled (lines) surface-flow velocities for the slow- and fast-flow periods of summer 1998.

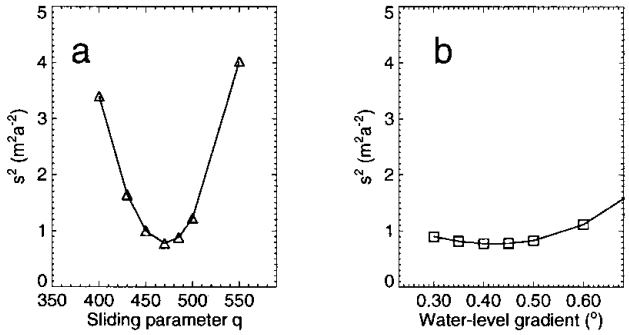

Fig. 6. Sensitivity of the model to parameter adjustment done by least-squares matching of modeled and measured velocities for the slow-flow scenario. The vertical axis shows the mean square error s^2 of the modeled and measured velocities. In (a) the mean square error is shown as a function of the sliding parameter q and a constant water-level gradient (0.45°). In (b) the mean square error is shown as a function of the water-level gradient and a constant sliding parameter ($q = 470$).

MODEL RESULTS AND COMPARISON WITH OBSERVATIONS

For the 1998 surface geometry, the model was run with various sliding scenarios. The results are shown in Figure 5 and discussed in this section.

Constant sliding coefficient

First, we set $c(x) = 0$, which corresponds to ice flow without sliding. The calculated surface velocities from internal deformation of the ice are much smaller than the observed values (Fig. 5). According to the observations, the surface velocities start to increase 4 km behind the calving front. From the difference between modeled velocities with $c(x) = 0$ and measurements, we estimate the amount of basal sliding to be about 3 times the deformation velocity in the upper part and to increase up to 20 times immediately behind the front. With a constant sliding coefficient, $c(x) > 0$, the surface velocity can be increased by nearly a constant value (Fig. 5), but the modeled velocity increase is limited to the frontmost 300 m. It follows that the observed surface velocity distribution cannot be explained with a constant sliding coefficient.

Spatially dependent sliding coefficient

To provide a spatially dependent $c(x)$ we introduce the effective pressure as suggested in Equation (7) into the sliding law (Equation (2)). Since the basal water pressure during the velocity measurements is not known, test scenarios need to be assumed. The basal water pressure behind a calving front must be at least equal to the pressure of the vertical water column at the calving face. During the melt season, the basal water pressure increases above this minimal pressure to force water to flow toward the front. Because our observations identified periods of fast flow and slow flow (Fig. 2), we select two different flow periods for the model calculations.

Slow-flow period

The observed velocities for this period correspond to the mean measured velocities of the period 31 July–8 August 1998. The sliding parameter q and the water-level gradient are adjusted to fit the velocity measurements with the method of least-squares matching (Fig. 6). The resulting water-level gradient is 0.45°, as shown in Figure 5. This seems a reasonable value, but Figure 6 shows that the model is not sensitive to small changes in the water-level gradient. The model results are shown in Figure 5 and are in good agreement with the observed velocities. The velocity increase, starting 4 km behind the front, is well reproduced by the model.

Fast-flow period

The fast-flow velocities correspond to the mean measured velocities of the period 12–15 July 1998. The sliding parameter q is the same as for the slow-flow scenario. By increasing the water level at the front by 17 m, and the water-level gradient to 1.79°, we get the best fit to observations (least-squares matching).

This higher water level takes into account the observed increased meltwater production and observed water outflow under high pressure at the lateral part of the calving front. In the upper 11 km we assume a reduced water-level gradient of 0.5°, to take into account the smaller surface slope in the upper part of the glacier. The modeled velocities are in good agreement with the measurements; the frontal increase in flow velocity is especially well reproduced (Fig. 5). The rather good agreement for stakes 1 and 2 suggests that the assumed reduced water-level gradient for the upper 11 km is reasonable, at least for the region where stakes 1 and 2 are located. Using the same sliding parameter as adjusted for the slow-flow scenario, the model is able to simulate the fast-flow situation if we increase the water level accordingly.

Highly crevassed zone

The frontmost 500 m of Hansbreen are highly crevassed. The formation of these crevasses is related to the stress field, which

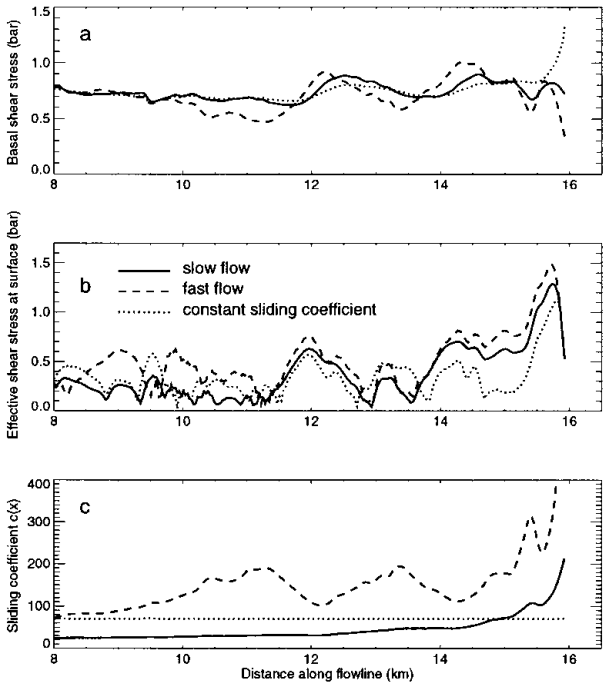

Fig. 7. (a) Basal shear traction along the flowline from model calculations. (b) Effective shear stress at the surface along the flowline from model calculations. (c) Sliding coefficient of the model along the flowline.

is also calculated in the flow model used. The modeled effective stress τ_{eff} at the surface is particularly large over a distance of 500 m immediately behind the calving front (Fig. 7). It exceeds 1 bar in all modeled scenarios. If we consider a "Von Mises criterion" for the formation of crevasses corresponding to an effective stress of >1 bar (Vaughan, 1993), the observed extent and location of the crevasse zone are in good agreement with the calculated high values of the effective stress.

CONCLUSION

Surface velocity measurements suggest that basal sliding processes play an important role in the dynamics and calving of tidewater glaciers, and need to be considered in the ice-flow modeling. It is shown that a sliding law dependent on basal shear stress can be successfully implemented in the finite-element glacier-flow model by adding a thin soft layer with variable viscosity at the base of the model. Results from model calculations with a constant or zero sliding coefficient show a frontal velocity increase only over a distance of 300 m (2–5 times the frontal ice thickness) instead of the observed 4 km. By using a sliding law which relates the sliding coefficient, and thus the basal velocity, to effective basal pressure, the model results reasonably reproduce the observed velocity increase behind the calving front. We conclude that basal sliding processes which strongly depend on the effective pressure dominantly control the flow of a grounded calving glacier like Hansbreen.

ACKNOWLEDGEMENTS

We thank J. Jania of the Geomorphological Institute of the University of Silesia, Poland. He made this field investigation on Hansbreen possible and helped greatly in the field. The Geophysical Institute of the Polish Academy of Science provided the infrastructure of the Polish polar station in Hornsund during the field investigation. The work was supported by Eidgenössische Technische Hochschule grant No. 0-20-400-97. R. A. Bindschadler and E. G. Josberger reviewed the manuscript and helped to improve it substantially.

REFERENCES

Alley, R. B., D. D. Blankenship, S. T. Rooney and C. R. Bentley. 1987. Till beneath Ice Stream B. 4. A coupled ice–till flow model. *J. Geophys. Res.*, **92**(B9), 8931–8940.

Bindschadler, R. 1983. The importance of pressurized subglacial water in separation and sliding at the glacier bed. *J. Glaciol.*, **29**(101), 3–19.

Boulton, G. S. and R. C. A. Hindmarsh. 1987. Sediment deformation beneath glaciers: rheology and geological consequences. *J. Geophys. Res.*, **92**(B9), 9059–9082.

Budd, W. F., P. L. Keage and N. A. Blundy. 1979. Empirical studies of ice sliding. *J. Glaciol.*, **23**(89), 157–170.

Colinge, J. 1998. Analyse numérique de la mécanique des glaciers dans un état stationnaire. (Thèse de doctorat, Université de Genève, No. 3001.)

Fowler, A. C. 1987. Sliding with cavity formation. *J. Glaciol.*, **33**(115), 255–267.

Funk, M. and H. Bösch. 1990. Gletscher-Kalbungsgeschwindigkeit im Süsswasser: eine Studie am Nordbogletscher im Johan Dahl Land, Süd-West Grönland. *Eidg. Tech. Hochschule, Zürich. Versuchsanst. Wasserbau, Hydrol. Glaziol. Ber.* 20.8, 1–47.

Giżejewski, J. 1997. Bottom morphology of the Hans Glacier forefield (Hornsund, south-west Spitsbergen, Svalbard). Preliminary report. *In* Głowacki, P., *ed. Polish Polar Studies, 24th Polar Symposium.* Warszawa, Polish Academy of Sciences. Institute of Geophysics, 63–69.

Glazovskiy, A. F., L. Kolondra, M. Yu. Moskalevskiy and J. Jania. 1991. Issledovaniya prilivnogo lednika Khansa na Shpitsbergene [Studies of the tide-water glacier Hansbreen on Spitsbergen]. *Mater. Glyatsiol. Issled.* 71, 143–149.

Hutter, K. 1983. *Theoretical glaciology; material science of ice and the mechanics of glaciers and ice sheets.* Dordrecht, etc., D. Reidel Publishing Co.; Tokyo, Terra Scientific Publishing Co.

Iken, A. 1978. Variations of surface velocities of some Alpine glaciers measured at intervals of a few hours. Comparison with Arctic glaciers. *Z. Gletscherkd. Glazialgeol.*, **13**(1/2), 1977, 23–35.

Iken, A. 1981. The effect of the subglacial water pressure on the sliding velocity of a glacier in an idealized numerical model. *J. Glaciol.*, **27**(97), 407–421.

Iken, A. and M. Truffer. 1997. The relationship between subglacial water pressure and velocity of Findelengletscher, Switzerland, during its advance and retreat. *J. Glaciol.*, **43**(144), 328–338.

Iverson, N. R., T. S. Hooyer and R. W. Baker. 1998. Ring-shear studies of till deformation: Coulomb-plastic behavior and distributed strain in glacier beds. *J. Glaciol.*, **44**(148), 634–642.

Jania, J. 1988. *Dynamiczne procesy glacjalne na poludniowym Spitsbergenie w świetle badań fotointerpretacyjnych i fotogrametrycznych [Dynamic glacial processes in south Spitsbergen in the light of photointerpretation and photogrammetric research].* Katowice, Uniwersytet Slaski. (Prace Naukowe Uniwersytetu Ślaskiego w Katowicach 955.)

Jania, J. and M. Kaczmarska. 1997. Hans Glacier — a tidewater glacier in southern Spitzbergen: summary of some results. *Byrd Polar Res. Cent. Rep.* 15, 95–104.

Jania, J. and L. Kolondra. 1982. *Field investigations performed during the glaciological Spitsbergen expedition in the summer of 1982: interim report.* Sosnowiec, Poland, Uniwersytetu Slaskiego. Instytut Geografii.

Jansson, P. 1995. Water pressure and basal sliding on Storglaciären, northern Sweden. *J. Glaciol.*, **41**(138), 232–240.

Kamb, B., H. Engelhardt, M. A. Fahnestock, N. Humphrey, M. Meier and D. Stone. 1994. Mechanical and hydrologic basis for the rapid motion of a large tidewater glacier. 2. Interpretation. *J. Geophys. Res.*, **99**(B8), 15,231–15,244.

Krimmel, R. M. and B. H. Vaughn. 1987. Columbia Glacier, Alaska: changes in velocity 1977–1986. *J. Geophys. Res.*, **92**(B9), 8961–8968.

Leysinger, G. 1998. Numerisches Blockgletschermodell in zwei Dimensionen. (Diplomarbeit Thesis, Eidgenössische Technische Hochschule, Zürich. Versuchsanstalt für Wasserbau, Hydrologie und Glaziologie.)

Lliboutry, L. 1968. General theory of subglacial cavitation and sliding of temperate glaciers. *J. Glaciol.*, **7**(49), 21–58.

Lliboutry, L. 1979. Local friction laws for glaciers: a critical review and new openings. *J. Glaciol.*, **23**(89), 67–95.

MacAyeal, D. R. 1989. Large-scale ice flow over a viscous basal sediment: theory and application to Ice Stream B, Antarctica. *J. Geophys. Res.*, **94**(B4), 4071–4087.

MARC Analysis Research Corp. 1997. *MARC/MENTAT user's manual. K7 edition.* Palo Alto, CA, MARC Analysis Research Corporation.

Meier, M. F. 1994. Columbia Glacier during rapid retreat: interactions between glacier flow and iceberg calving dynamics. *In* Reeh, N., *ed. Report of a Workshop on "The Calving Rate of the West Greenland Glaciers in Response to Climate Change", Copenhagen, 13–15 September 1993.* Copenhagen, Danish Polar Center, 63–83.

Meier, M. *and 9 others.* 1994. Mechanical and hydrologic basis for the rapid motion of a large tidewater glacier. 1. Observations. *J. Geophys. Res.*, **99**(B8), 15,219–15,229.

Paterson, W. S. B. 1994. *The physics of glaciers. Third edition.* Oxford, etc., Elsevier.

Rott, H., M. Stuefer, A. Siegel, P. Skvarca and A. Eckstaller. 1998. Mass fluxes and dynamics of Moreno Glacier, Southern Patagonia Icefield. *Geophys. Res. Lett.*, **25**(9), 1407–1410.

Van der Veen, C. J. 1996. Tidewater calving. *J. Glaciol.*, **42**(141), 375–385.

Vaughan, D. G. 1993. Relating the occurrence of crevasses to surface strain rates. *J. Glaciol.*, **39**(132), 255–266.